Isotope Studies of Photocatalysis: Dual Mechanisms in the Conversion of Anisole to Phenol

Xiaojing Li and William S. Jenks*

Contribution from the Department of Chemistry, Iowa State University, Ames, Iowa 50011-3111

Received November 15, 1999. Revised Manuscript Received October 3, 2000

Abstract: The partial TiO_2-mediated photocatalytic degradation of anisole has been studied using isotopically labeled substrates and comparisons to Fenton and $h\nu/H_2O_2$ chemistry. An H/D isotope selectivity of 2.7 is observed for hydrogen abstraction from the methyl group in all cases. An ^{18}O tracer study shows that anisole is simultaneously converted to phenol by both *ipso* attack and degradation of the methyl. The isotope selectivity for hydroxylation of anisole is reported to be about 1.3 under all conditions. This is attributed to an O_2-dependent competition along the reaction pathway that can be avoided by use of benzoquinone instead of O_2 as an electron acceptor with TiO_2. Under those conditions, the H/D isotope selectivities are between 0.9 and 1.0, as would be expected for inverse secondary kinetic isotope effects.

Introduction

Titanium dioxide mediated photocatalytic degradation of organic compounds in aerated water leads to their complete mineralization, that is, oxidation to CO_2, H_2O, and other inorganic ions.[1−7] It is thus an attractive technology for certain water purification applications. The initial event in photocatalytic degradation is charge separation within the semiconductor particle, induced by absorption of near-UV light. Superoxide ($O_2^{\bullet-}$) is formed by rapid electron transfer to molecular oxygen, which prevents rapid charge recombination within the TiO_2 particle. The remaining valence band hole can oxidize water to give an adsorbed hydroxyl radical and a proton or oxidize an adsorbed organic substrate directly by single electron transfer (SET).

Much of the degradative chemistry has been attributed to reactions of surface bound hydroxyl radicals with the organics, but some products appear to derive from reactions of the SET-oxidized organic compound.[8−21] In particular, we have recently been concerned with the chemical mechanisms by which aromatic molecules are degraded. Ring opening of benzene moieties appears to be driven by SET-derived chemistry, but only after two or three oxygenations of the ring. Other reactions, such as degradation of alkyl substituent moieties, hydroxylation of unsubstituted aryl positions, and aryl substitution reactions are all processes that occur in competition "early" in the degradations and are usually attributed to hydroxyl radical chemistry.

A mechanistic issue of interest is the manner in which substituents are lost: by attack on the arene or by degradation of the exterior alkyl substituent, i.e., is degradation of the alkyl or related stubstituents typically faster than, slower than, or competitive with reactions at the arene portion. The first steps of both types of process, addition to aromatic rings and hydrogen abstraction from alkyl positions, are well-known reactions of $HO^{\bullet}$. Conversion of chloroarenes to phenols occurs by *ipso* attack of $HO^{\bullet}$ [22] on the aromatic ring, but the situation is less clear for other substituents.[23] For example, alkoxy substituents in particular could be "substituted for" or could have the alkyl portion degraded away; both paths lead to phenols.

We report here a study of the initial steps of photocatalytic degradation of anisole, examining both its hydroxylation and its conversion to phenol. It was chosen as the simplest model with which reactions of alkoxyarenes could be examined, and one in which $HO^{\bullet}$-mediated chemistry was expected to dominate over SET-induced chemistry based on our previous experi-

(1) Pelizzetti, E.; Serpone, N. *Homogeneous and Heterogeneous Photocatalysis*; D. Reidel Publishing Company: Boston, MA, 1986.
(2) Serpone, N.; Pelizzetti, E. *Photocatalysis: Fundamentals and Applications*; John Wiley & Sons: New York, 1989.
(3) Helz, G. R.; Zepp, R. G.; Crosby, D. G. *Aquatic and Surface Photochemistry*; Lewis Publishers: Boca Raton, FL, 1994.
(4) Fox, M. A.; Dulay, M. T. *Chem. Rev.* **1993**, *93*, 341−357.
(5) Linsebigler, A. L.; Lu, G.; Yates, J. T., Jr. *Chem. Rev.* **1995**, *95*, 735−758.
(6) Stafford, U.; Gray, K. A.; Kamat, P. V. *Heterog. Chem. Rev.* **1996**, *3*, 77−104.
(7) Schiavello, M. *Heterogeneous Photocatalysis*; Wiley: New York, 1997.
(8) Li, X.; Cubbage, J. W.; Tetzlaff, T. A.; Jenks, W. S. *J. Org. Chem.* **1999**, *64*, 8509−8524.
(9) Li, X.; Cubbage, J. W.; Jenks, W. S. *J. Org. Chem.* **1999**, *64*, 8525−8536.
(10) Cermenati, L.; Pichat, P.; Guillard, C.; Albini, A. *J. Phys. Chem. B* **1997**, *101*, 2650−2658.
(11) Amalric, L.; Guillard, C.; Pichat, P. *Res. Chem. Intermed.* **1994**, *20*, 579−594.
(12) Theurich, J.; Bahnemann, D. W.; Vogel, R.; Ehamed, F. E.; Alhakimi, G.; Rajab, I. *Res. Chem. Intermed.* **1997**, *23*, 247−274.
(13) Maillard-Dupuy, C.; Guillard, C.; Courbon, H.; Pichat, P. *Environ. Sci. Technol.* **1994**, *28*, 2176−2183.
(14) Maillard-Dupuy, C.; Guillard, C.; Pichat, P. *New J. Chem.* **1994**, *18*, 941−948.
(15) Piccinini, P.; Minero, C.; Vincenti, M.; Pelizzetti, E. *Catal. Today* **1997**, *39*, 187−195.
(16) Minero, C.; Mariella, G.; Maurino, V.; Pelizzetti, E. *Langmuir* **2000**, *16*, 2632−2641.
(17) Sahyun, M. R. V.; Serpone, N. *J. Photochem. Photobiol. A* **1998**, *115*, 231−238.
(18) Galindo, C.; Jacques, P.; Kalt, A. *J. Photochem. Photobiol. A* **2000**, *130*, 35−47.
(19) Guillard, C. *J. Photochem. Photobiol. A* **2000**, *135*, 65−75.
(20) Soana, F.; Sturini, M.; Cermenati, L.; Albini, A. *J. Chem. Soc., Perkin Trans. 2* **2000**, 699−704.
(21) Cermenati, L.; Albini, A.; Pichat, P.; Guillard, C. *Res. Chem. Intermed.* **2000**, *26*, 221−234.
(22) The use of the term "$HO^{\bullet}$" is elaborated in the Discussion section.
(23) Stafford, U.; Gray, K. A.; Kamat, P. V. *J. Phys. Chem.* **1994**, *98*, 6343−51.

10.1021/ja994030h CCC: $19.00
Published on Web 11/11/2000

ence.[8,9] We show that phenol is formed competitively by both (a) the substitution reaction of HO for CH_3O beginning with *ipso* attack and (b) the degradation of the methyl group beginning with hydrogen abstraction. Additionally, we use isotopic labels to examine the hydroxylation and hydrogen abstraction reactions that occur in various positions.

This finding of a substitution mechanism for the conversion of RO to HO stands in contrast to previous results for cyanuric acid derivatives. The common herbicide atrazine (6-chloro-*N*-ethyl-*N*′-isopropyl[1,3,5]triazine-2,4-diamine) is degraded to cyanuric acid but no further.[24−26] We have recently shown that model alkoxytriazines are converted to cyanuric acid without attack at the ring and that TiO_2-mediated exchange of the oxygen atoms is very slow if it occurs at all.[27]

Experimental Section

Materials. Anisole (**1**), anisole-d_3 ($C_6H_5OCD_3$), and anisole-d_8 were used as received from Aldrich. Anisole-d_5 ($C_6D_5OCH_3$) was prepared by the reaction of phenol-d_6 with CH_3I in the presence of K_2CO_3 and acetone. ^{18}O-enriched anisole was prepared by the reaction of CH_3I with ^{18}O-enriched phenol, which was prepared as described by Winkel.[28] Phenyl formate was prepared according to the method described by Stevens.[29] The water employed was purified by a Milli-Q UV plus system (Millipore) resulting in a resistivity more than 18 MΩ cm^{-1}. TiO_2 was Degussa P-25, which consists of 75% anatase and 25% rutile with a specific BET surface area of 50 m^2 g^{-1} and a primary size of 20 nm.[30] Other chemicals were obtained from Aldrich as the highest grade available and purified as necessary.

Photocatalytic Degradations. Samples containing the desired concentration of anisole and 50 mg of suspended TiO_2 were prepared in water (80 mL). Three types of runs were carried out. Kinetics runs were analyzed by HPLC and the initial concentration of anisole was 2.0 mM. Product distribution runs were analyzed by GC, and the initial concentration of anisole was 4.0 mM. For isotope selectivity runs using a pair of anisole isotopomers, total initial concentrations were 1−5 mM, while the ratio of one anisole isotopomer to the other was varied from run to run. Products were again analyzed by GC. When used (as noted in the table entries), the initial concentration of benzoquinone (BQ) was 10 mM.

Degradations were carried out at a variety of pH values. Between pH 4.0 and 8.7, 1 mM phosphate buffer was used, and pH 10.8 was maintained with 25 mM phosphate buffer. The pH 1 and 2 solutions were obtained by adding perchloric acid.

Prior to irradiation, each mixture was treated in an ultrasonic bath for 5 min to disperse larger aggregates of TiO_2 and then purged with O_2 (or Ar as noted) for 20 min in the dark. The samples were sealed with a rubber septum and the headspace (∼90 cm^3) was filled with O_2 (or Ar, as appropriate). Irradiations were carried out at 25 ± 2 °C in a Rayonet photochemical minireactor equipped with a magnetic stirring device and a fan. Light was provided by 8 × 4 W "black light" bulbs whose emission was centered at 360 nm. Control experiments showed that anisole did not degrade on the time scale of the experiments if any one of the components of the mixtures or light was not present.

HPLC Analysis of Kinetic Runs. Samples of approximately 0.5 mL were taken through the septum by syringe before photolysis and at regular intervals during the irradiation. They were filtered using syringe-mounted 0.2 μm Millipore filters before HPLC analysis. The concentrations of anisole, phenol, 2-methoxyphenol, and 4-methoxyphenol were measured by HPLC using a HP 1050 HPLC with diode array UV/vis detection and an ODS Hypersil C_{18} reverse phase column (5 μm loop, 200 × 2.1 mm). Substances were routinely quantified from their absorbance at 220 nm. The eluent was 15% aqueous methanol and the flow rate was 0.5 mL min^{-1}. First-order decays were obtained from plots of concentration of anisole vs time. Relative standard errors of the fits were all <5% and absolute time constant values from independent runs were reproducible to within 10%. The relative rates are of the greatest significance, since the absolute rates are functions of light intensity, sample geometry, etc.

Table 1. Relative Yields of Products Formed by TiO_2-Mediated Photocatalytic Degradation, H_2O_2 Photolysis, and Fenton Reactions[a]

			relative yield					
entry	conditions	pH	**2**	**3**	(^{18}O)[b]	**4**	**5**	**6**
1	$h\nu + TiO_2 + O_2$	1.0	28	68	(31)	3	1	
2		2.0	27	43		18	9	4
3		4.0	16	30	(19)	27	26	1
4		7.0	6	24	(17)	29	40	1
5		8.7	1	23		32	44	
6		10.8	0	44	(29)	34	13	9
7	$h\nu + TiO_2 + BQ$	1.0	0	15		62	23	0
8		7.0	0	8	(19)	53	36	3
9	$h\nu + TiO_2$	7.0	0	90		7	2	1
10	$h\nu + H_2O_2 + O_2$	1.0	69	21		4	5	2
11		7.0	3	22	(14)	48	23	1
12	$h\nu + H_2O_2$	1.0	69	36		2		
13		7.0	0	24		55	17	4
14	$Fe^{2+} + H_2O_2 + O_2$	1.0	62	33			5	
15		7.0	1	22	(16)	45	27	5
16	$Fe^{2+} + H_2O_2$	1.0	33	66				
17		7.0	0	18		46	32	4

[a] All entries were from at least duplicate runs, except the ^{18}O abundance of phenol. [b] ^{18}O percentage in **3** when starting material **1** contains 71.6% ^{18}O.

GC-MS of Product Distributions and Isotope Selectivity Runs. After reactions were stopped, the solutions were acidified to pH 2.5 and filtered if necessary, then extracted with ether four times. The ether solutions were dried with $MgSO_4$ and concentrated to 1 mL. The concentrated sample was directly injected. 4-Methylbenzyl alcohol was used as an internal standard for integration by addition after the reaction. The GC-MS analyses were carried out on a Finnigan Magnum ion trap mass spectrometer equipped with a 30 m DB-5 column. A HP 5890 series II Gas Chromatograph with 30 m ZB-5 and FID detection was used for routine work.

Entries in Table 1 are based on at least two independent runs and multiple GC shots for each run. Run-to-run reproducibility was better than 10% relative error. Some of the ^{18}O abundance runs were only carried out once.

Entries in Table 2 are based on integration of the separated GC peaks, including product isotopomers, which were also separable by GC. Response factors for the commercial isotopomers of anisole were all within 1% of each other and thus it was assumed that all isotopomer pairs would also have identical response factors. All reported values in Table 2 represent at least duplicate shots. The total range of product ratios for several GC shots never exceeded 5% of the reported value. Seven independent runs of different ratios of **1** and **1-d8** were performed at pH 7, all yielding nearly identical selectivity values. For other conditions, fewer runs were carried out. A complete table of all runs is available as part of the Supporting Information.

H_2O_2 Photolysis. Solutions were prepared as above, leaving out the TiO_2. Immediately before photolysis 1.0 mL of H_2O_2 (30% in water) was added. The mixtures were irradiated with 8 × 4 W lamps whose emission is centered at 300 nm. Analyses were done as previously described.

Fenton Reactions. Reactions were conducted at room temperature. Normal conditions were 4 mM anisole, 8 mM $FeSO_4$, and 80 mM H_2O_2. The pH of the solution was adjusted with H_2SO_4 for runs at pH 1, and with phosphate buffer (0.1 M) for runs at pH 7. Analyses were done as previously described.

(24) Minero, C.; Maurino, V.; Pelizzetti, E. *Res. Chem. Intermed.* **1997**, *23*, 291−310.
(25) Pelizzetti, E.; Maurino, V.; Minero, C.; Carlin, V.; Pramauro, E.; Zerbinati, O.; Tosato, M. L. *Environ. Sci. Technol.* **1990**, *24*, 1559−1565.
(26) Yue, P. L.; Allen, D. Photocatalytic Degradation of Atrazine. In *Photocatalytic Purification and Treatment of Water and Air*; Ollis, D. F., Al-Ekabi, H., Eds.; Elsevier: New York, 1993; Vol. 3, pp 607−611.
(27) Tetzlaff, T.; Jenks, W. S. *Org. Lett.* **1999**, *1*, 463−465.
(28) Winkel, C.; Aarts, M. W. M. M.; Van der Heide, F. R.; Buitenhuis, E. G.; Lugtenburg, J. *Recl. Trav. Chim. Pays-Bas* **1989**, *108*, 139−146.
(29) Sevens, W.; Van Es, A. *Recl. Trav. Chim.* **1964**, *83*, 1294−1298.
(30) DeGussa *DeGussa Technol. Bull.* **1984**, *56*, 8.

Table 2. the Isotope Selectivity Ratios Observed on Degradations of Isotopomeric Mixtures of **1**

entry	starting materials	conditions	pH	isotope selectivity 2	3	4	5
1	**1**, **1-d8**	*hν*, TiO_2, O_2	1.0	2.48	1.35	1.27	1.30
2			2.0	2.54	1.43	1.17	1.46
3			4.0	2.62	1.27	1.20	1.07
4			7.0[a]	2.73	1.30	1.31	1.17
5			8.5	2.80	1.34	1.35	1.19
6		h*ν*, TiO_2, BQ[b]	7.0		1.31	0.94	0.98
7		Fe^{2+}, H_2O_2, O_2 [b]	7.0	2.72	1.15	1.11	1.08
8		*hν*, H_2O_2, O_2 [b]	7.0	2.70	1.14	1.30	1.04
9		*hν*, H_2O_2 [b]	7.0		1.34	0.95	0.94
10	**1**, **1-d5**	*hν*, TiO_2, O_2	7.0	1.04	0.98	1.30	
11		Fe^{2+}, H_2O_2, O_2 [b]	7.0	1.01	0.96	1.09	
12	**1-d3**, **1-d5**	*hν*, TiO_2, O_2	7.0	2.71	1.31		
13		Fe^{2+}, H_2O_2, O_2 [b]	7.0	2.39[c]	1.29		
14	**1-d3**, **1-d8**	*hν*, TiO_2, O_2	7.0	0.96	1.06		
15		Fe^{2+}, H_2O_2, O_2	7.0	1.01	0.99		

[a] Average of seven independent runs under different ratios of **1**/**1-d8** of 0.44 to 3.03. Standard deviations of all ratios are ±0.03. [b] Average of two runs. [c] Subject to larger error because of small quantities of product.

Results

The oxidation of anisole has been studied previously under pulse radiolysis,[31−33] Fenton,[34] and other conditions,[35−37] but not by photocatalysis. Here, partial degradations of anisole and several isotopomers were carried out using TiO_2-mediated photocatalysis, the Fenton reaction, and hydrogen peroxide photolysis. The latter two sets of conditions were used as control studies to characterize the TiO_2 chemistry. In general, the results of all three sets of degradation conditions were very similar (vide infra), and this was taken as evidence that the TiO_2-mediated degradations were initiated mainly by adsorbed $HO^{\bullet}$, not hole oxidation. This result is consistent with our previous and continuing work with similar substrates.[8,9]

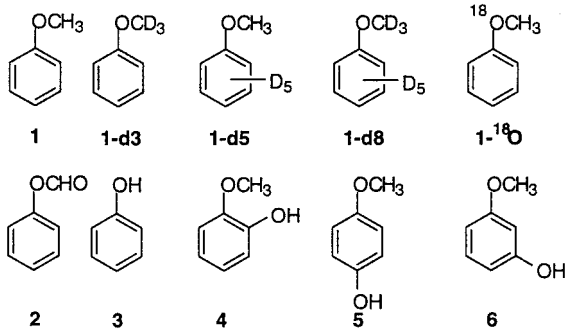

Photocatalytic degradations were carried out in O_2-saturated aqueous solutions at several pH values. Three different types of measurements were made. Kinetics of degradation as a function of pH were obtained using periodic sampling and HPLC detection. Product distributions were determined by GC analysis of runs designed from the kinetic information, and finally, mixtures of **1** and the illustrated isotopomers were degraded to determine H/D selectivities for the formation of products **2**−**6**.

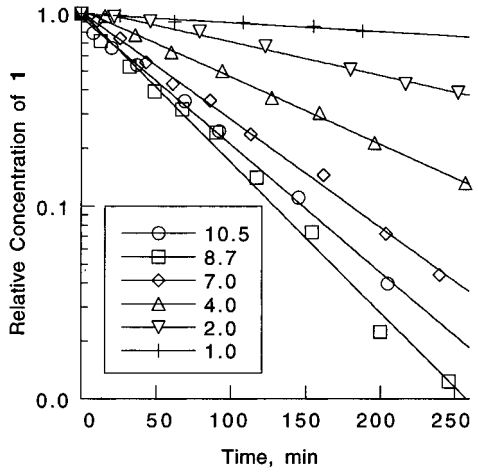

Figure 1. Rates of degradation of **1** as a function of pH. The initial concentrations were ca. 2.0 mM. See text for details of buffers.

Kinetics Runs. To design conditions with which to study the initial product distributions of the degradations, kinetics runs were carried out. The rate of degradation of a given organic substrate is expected to vary with pH because of the changing surface charge on the TiO_2, the change in adsorption characteristics of the organics, and other factors. Usually, degradation is faster at higher pH.[6] Because photocatalytic degradations inherently create acid, buffers are generally required to study pH effects, and were used here except at the lowest pH values.

The rate of decay of **1** and the buildup and decay of several products were followed by HPLC analyses of photocatalytic degradations. As illustrated in Figure 1, the disappearance of **1** was exponential over at least 2−3 half-lives. The rate of decay increased almost linearly with pH until a dip from pH 8.8 to 10.8. Similar correlations have been observed previously for hydroquinone and other aromatic systems.[6,8,38]

In addition to decay of **1**, the buildup and loss of several degradation intermediates were monitored. By HPLC, only compounds **3**−**5** were uniquely identified as products. (In GC-detected runs described below, primary degradation products **2** and **6** were also uniquely identified.) Additional small, fast-running (polar) HPLC peaks that have been shown[8,9] to include multiple acyclic acids and/or polyhydroxylated aromatics were also observed, but were taken to represent downstream degradation. The concentrations of **3**−**5** as a function of time for a pH 7 solution are given in Figure 2.

Determination of Primary Product Distributions. On the basis of data in Figures 1 and 2, 30 min was chosen as a standard degradation time that would yield a representative initial primary product distribution. The results of these reactions are given in Table 1, which only lists the major primary products. Analyses carried out by GC and GC-MS showed other trace compounds in the mixtures: di- and trihydroxylated species and ring-opened compounds.[8,9] Phenyl formate (**2**) has not been reported previously as an anisole degradation product, but its analogue has been observed in the degradation of more highly substituted cases.[39] It should be noted that **2** is subject to hydrolysis or secondary photocatalytic degradation to **3**. It is thus assumed that the values in Table 1 are lower limits on the actual proportion of **2** formed.

(31) Fang, X.; Pan, X.; Rahmann, A.; Schuchmann, H.-P.; von Sonntag, C. *Chem. Eur. J.* **1995**, *1*, 423−429.
(32) Steenken, S.; Raghavan, N. V. *J. Phys. Chem.* **1979**, *83*, 3101−3107.
(33) Eberhardt, M. K. *J. Phys. Chem.* **1977**, *81*, 1051−1057.
(34) Kurata, T.; Watanabe, Y.; Katoh, M.; Sawaki, Y. *J. Am. Chem. Soc.* **1988**, *110*, 7472−7478.
(35) Jefcoate, C. R. E.; Norman, R. O. C. *J. Chem. Soc. B* **1968**, 48−53.
(36) Perry, R. A.; Atkinson, R.; Pitts, J. N., Jr. *J. Phys. Chem.* **1977**, *81*, 1607−1611.
(37) O'Neill, P.; Schulte-Frohlinde, D.; Steenken, S. *J. Chem. Soc., Faraday Discuss.* **1977**, *63*, 141−148.
(38) Djebbar, K.; Sehili, T. *Pestic. Sci.* **1998**, *54*, 269−276.
(39) Guillard, C.; Amalric, L.; D'Oliveira, J.-C.; Delprat, H.; Hoang-Van, C.; Pichat, P. *Aquat. Surf. Photochem.* **1994**, 369−386.

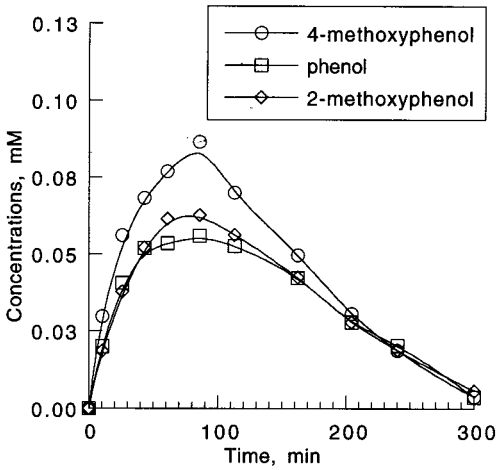

Figure 2. Concentrations of intermediate degradation products from photocatalytic degradation of anisole. Initial conditions: 2.0 mM anisole, 5 mM phosphate buffer, pH 7, 50 mg of TiO_2 in 80 mL. The decay rate of **1** is 0.0128 min^{-1}.

The product distributions were sensitive to pH. Phenol and its formate ester predominate at low pH, but the proportion of *ortho* and *para* hydroxylation to give **4** and **5** rises until pH 8.7. Concomitant with the drop in the reaction rate, the proportion of **4** and **5** drops again at the highest pH.

In a few runs, benzoquinone (BQ) was used as an electron acceptor in lieu of O_2, an idea taken from the result that BQ is reduced to hydroquinone in the absence of O_2 under photocatalytic conditions.[40,41] In good accord with radiolysis experiments in the presence of BQ,[32] hydroxylation dominates the product distribution, even at low pH.

Degradations using Other Conditions. To compare with the TiO_2-mediated photocatalytic degradation, photolysis of O_2-saturated solutions containing H_2O_2 were carried out, as were dark Fenton reactions with excess H_2O_2. Both were kept to low conversion of anisole, and the results of these experiments are shown in Table 1 as entries 10−13 and 14−17, respectively. The product distributions for the Fenton chemistry as a function of pH were in good conformity with a previous report.[35]

Isotope Selectivities. Isotope selectivities were viewed as a method to examine the mechanism(s) of the reactions. Reactions were carried out at approximately 4 mM total concentration of mixtures of the H/D isotopomers of **1**, using various ratios of the labeled and unlabeled materials. Most of the product isotopomers were separable by GC.[42]

The quantities of the products **2**−**5** that derived from each isotopomer were determined from the GC runs. Selectivities, shown in Table 2, were obtained by dividing the observed isotopomer ratios of the products by the initial isotopomeric ratio of the anisole. A version of Table 2 that lists each run with its individual ratio of anisole isotopomers is available in the Supporting Information.

In several degradation runs, anisole that had been enriched in ^{18}O (**1-^{18}O**) was used. Its initial isotopic enrichment was 72% as determined by mass spectrometry. The isotopic enrichment of the products under various conditions was examined. The enrichment of **2** and **4**−**6** remained at 72% within a small experimental error under all conditions. The enrichment for phenol, however, varied and is reported in Table 1. Representative data are shown in Figure 3.

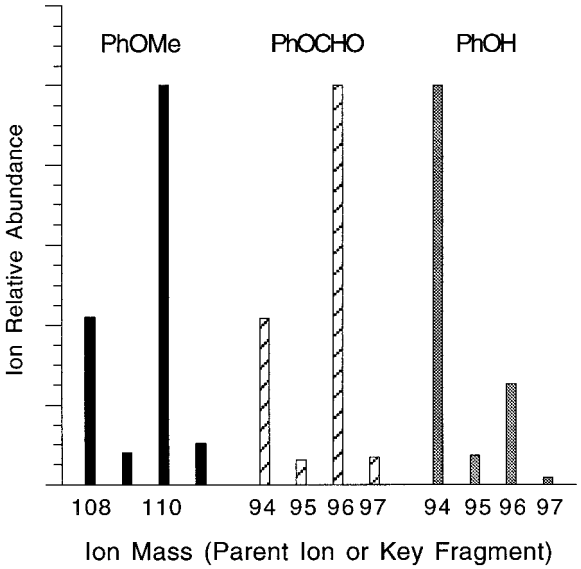

Figure 3. Ion relative abundance for determination of ^{18}O content. Normalized relative abundances were from a single GC-MS run after partial photocatalytic degradation at pH 7. The phenol fragment (base peak) was used for phenyl formate.

Discussion

Absorption of UV light by TiO_2 results in charge separation in the particle. To avoid rapid charge recombination and energy wasting, an electron acceptor is necessary; this role is usually filled by O_2. The remaining "hole" causes single electron oxidation of adsorbed substrates. Radical cations can be formed from organic substrates or surface-bound hydroxyl radicals may be formed. Because anisole is not strongly adsorbed to TiO_2 and because of the similarity of product distributions obtained from photocatalytic degradation, the Fenton reactions, and the hydrogen peroxide photolyses, the assumption is made throughout this discussion that all the photocatalytic degradation reactions considered here begin with species related to the adsorbed hydroxyl radical, rather than SET. Further, just as it has been argued that the oxidant in TiO_2-mediated photocatalytic degradation is not a free-floating hydroxyl radical, it has recently been argued that Fenton chemistry is distinct from free hydroxyl radical chemistry.[43] It is not our purpose here to argue the exact nature of the oxidizing agents in either of these conditions. The important notion to read from this is that the mode of reactivity in the photocatalytic conditions is that of the hydroxyl radical type, as opposed to the single electron-transfer type. For purposes of clarity, we will write the species as $HO^{\bullet}$, though it must be clear that this may include surface- or metal-bound species.

Multiple Mechanisms for Phenol Formation by Photocatalysis. Hydroxyl radical has a well-deserved reputation for addition reactions to aromatic rings, particularly with electron-rich systems, such as anisole. Indeed, the degradation of anisole with hydroxyl radicals produced by radiolysis seems to have been rationalized without consideration that $HO^{\bullet}$ might have reacted with the methyl group.[32] In contrast, a gas-phase study of anisole showed that at room temperature approximately 20% of the reactivity of $HO^{\bullet}$ with anisole was expected at the methyl position by extrapolation of the data.[36] The current results for photocatalytic degradation are more consistent with the latter interpretations, and lead to the conclusion that there are at least

(40) Richard, C. *New J. Chem.* **1994**, *18*, 443−445.
(41) Richard, C.; Boule, P. *New J. Chem.* **1994**, *18*, 547−52.
(42) The methoxyphenol selectivities are not reported for **1** vs **1-d3** and **1-d5** vs **1-d8** because of overlap problems in the GC runs.
(43) Sawyer, D. T.; Sobkowiak, A.; Matsushita, T. *Acc. Chem. Res.* **1996**, *29*, 409−416.

Scheme 1

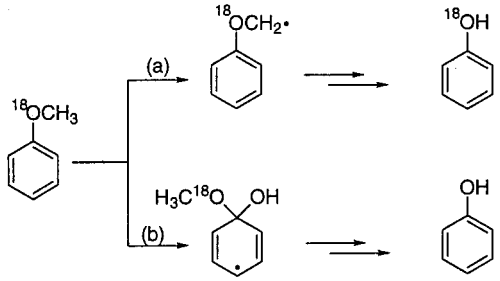

two mechanisms that lead to phenol formation. As illustrated in Scheme 1, we envision pathways that begin with attack at the methyl and with *ipso* attack on the aromatic ring.

We consider first path a), and suggest that phenyl formate (**2**) as well as phenol derives from it. Consistent with the formation of **2** beginning with attack at the methyl, there is no significant isotope effect for its formation from **1** vs **1-d5** (entries 10 and 11 in Table 2). Moreover, when **1-^{18}O** is used as starting material, the phenyl formate contains the same degree of enrichment as the starting material. Thus, postulating that formation of radical **7** is the initial step, trapping by O_2 provides the peroxyl radical **8**. The formate is obtained by disproportionation or reaction with $HO_2\bullet$ according to the Russell mechanism.[44,45] Consistent with this reaction sequence, **2** is not observed when benzoquinone is used as an alternate electron acceptor for O_2 in the TiO_2-mediated degradation (entries 7 and 8 in Table 1). The formation of **2** under the Fenton and H_2O_2 photolysis conditions without additional oxygen presumably comes about because of the formation of O_2 as a natural product of the conditions,[43,46] though other mechanisms cannot be ruled out.

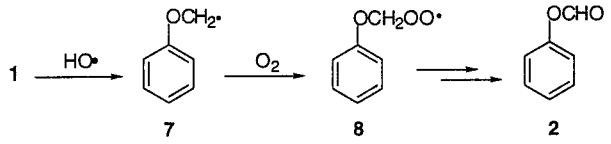

The H/D selectivity for formation of **2** is approximately 2.7, as shown by the various entries in Table 2. This selectivity is taken to reflect the H/D kinetic isotope effect in formation of radical **7**.[47] It is quite comparable for all three oxidation methods used here and implies that the transition states bear qualitative resemblance to one another (though there may be metal or semiconductor association of the hydroxyl species). This value of 2.7 is somewhat smaller than the 3.3 obtained for trimethyl cyanurate in comparable experiments,[27] but within the fairly wide range of 2−5 expected from other reported studies.[48−52]

Having established the existence of path a in Scheme 1, we consider path b. From Table 1, it can be seen that the ^{18}O-enrichment of phenol (**3**) varied, but was consistently below the 72% enrichment of the starting material **1-^{18}O**. Even including **2**, in which ^{18}O was fully retained, as "pre-**3**", the retention of ^{18}O does not exceed 60%. Attack of HO• on the *ipso* position accounts for loss of ^{18}O if the adduct **9** loses the elements of methanol. The formation of methanol in nearly equal proportion to phenoxyl radicals has been observed in radiolysis conditions.[37] The final hydrogen atom may be scavenged either directly from a source such as HOO• or by stepwise electron and proton transfer.

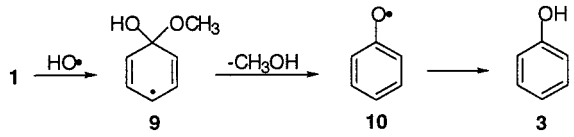

Entry 8 in Table 1 indicates that there are also two mechanisms for formation of phenol when BQ is used as the electron sink instead of O_2. While path b does not invoke O_2, we have postulated its involvement in path a. Yet just over a quarter of the phenol appears to be formed by attack at methyl, based on the partial retention of ^{18}O. There is no specific evidence for the mechanism of **3-^{18}O** formation. However, it is reasonable to hypothesize that **7** is oxidized to the cation, which is highly susceptible to hydrolysis to phenol. The greater yield of **3** under acidic conditions may be consistent with the greater oxidizing power of BQH^+, compared to BQ itself. Furthermore, the 19% abundance of ^{18}O in **3**, combined with an estimate of k_H/k_D for abstraction of the methyl hydrogens of 2.7 predicts an observed isotope selectivity of 1.3 for formation of **3**, in reasonable agreement with the observed value.

Anomalous Isotope Effects for 4 and 5. On first inspection, the H/D selectivity values for **3**−**5**, particularly those for **4** and **5**, are surprising. It is well-known that hydroxyl adds to aromatic rings, and an *inverse* secondary isotope effect is expected. In a gas-phase study, no kinetic isotope effect for benzene and benzene-d_6 was observed near room temperature,[53] though it is unclear whether the precision of these experiments would allow detection of an effect of just a few percent.[54]

The present selectivity values, which are greater than unity, require explanation. One reasonable rationalization is that there is an isotope-dependent branching point in the mechanism of product formation after the initial addition step. The isotope-dependent branch leads to products unaccounted for by observation of **4** and **5** and affects the apparent selectivity.

A related observation was made in radiolysis of benzene and benzene-d_6 in oxygenated water.[55] The ratio of *G*-values (efficiencies) of phenol formation from benzene and benzene-d_6 was 1.35. This was interpreted as outlined in Scheme 2.[55] After formation of the initial adduct and trapping by O_2 to give **11**, the elimination of HOO• to give phenol has a (unmeasured) primary isotope effect, but the pathway in which another oxygen molecule adds to the cyclized species to degrade to other compounds does not. (Two of the four possible isomers of **11** cannot undergo the elimination, but the addition of O_2 is reversible.[56]) Since the conversion of **11** to **3** is faster in the proteo case than in the deuterio case, less of the ^{1}H-**11** is diverted to the other products. This type of branching would distort the competition experiments reported here just as it affects the *G*-values in the radiolysis experiments. Dividing the H/D

(44) Russell, G. A. *J. Am. Chem. Soc.* **1957**, *79*, 3871−3877.
(45) Chuang, C.-C.; Chen, C.-C.; Lin, J.-L. *J. Phys. Chem. B* **1999**, *103*, 2439−2444.
(46) Walling, C. *Acc. Chem. Res.* **1975**, *8*, 125−131.
(47) It should also be noted that there may be pathways from **7** to **3** that bypass **2**. We have no specific evidence on this point.
(48) McCaulley, J. A.; Kelly, N.; Kaufman, F. *J. Phys. Chem.* **1989**, *93*, 1014−1018.
(49) Tully, F. P.; Droege, A. T. *J. Phys. Chem.* **1986**, *90*, 1949−1954.
(50) Tully, F. P.; Droege, A. T. *J. Phys. Chem.* **1986**, *90*, 5937−5941.
(51) Tully, F. P.; Droege, A. T. *J. Phys. Chem.* **1987**, *91*, 1222−1225.
(52) Tully, F. P.; Hess, W. P. *J. Phys. Chem.* **1989**, *93*, 1944−47.
(53) Lorenz, K.; Zellner, R. *Ber. Bunsen-Ges. Phys. Chem.* **1983**, *87*, 629−636.
(54) Above 420 K, an isotope effect was observed because hydrogen abstraction from benzene becomes a kinetically important route.
(55) Pan, X.-M.; Schuchmann, M. N.; von Sonntag, C. *J. Chem. Soc., Perkin Trans. 2* **1993**, 289−297.
(56) Pan, X.-M.; von Sonntag, C. *A. Naturforsch.* **1990**, *45b*, 1337−1340.

Scheme 2

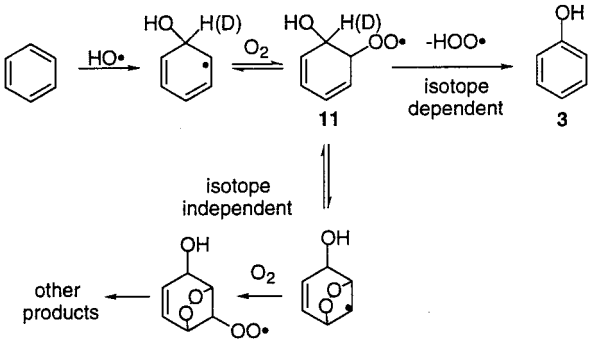

[a] Compound **11** is representative of both *ortho* and *para* trapping products.

selectivities of **3**−**5** in the oxygenated experiments (entries 1−5 and 7−11) by the factor of 1.35 would produce adjusted product ratios in line with expectations for an inverse secondary isotope effect.

The experiments using BQ instead of O_2 as an electron sink can be used to test this hypothesis. Noting that the isotope selectivities we had observed for photocatalytic degradation in the presence of oxygen for the formation of **4** and **5** were roughly the same as the reported $G(C_6H_6)/G(C_6D_6)$ ratio,[55] the experiments using BQ as a substitute for O_2 were carried out to eliminate the competition between an isotope-dependent and isotope-independent reaction of the initial hydoxyl adduct of anisole. Obviously, the mechanism for hydroxylation of anisole must change from that shown in Scheme 2 because of the lack of oxygen, but undoubtedly the first step is the same: formation of the HO• adduct on the aryl ring. After adduct formation, we presume that BQ oxidizes the radical to the cation, from which the methoxyphenol is formed.

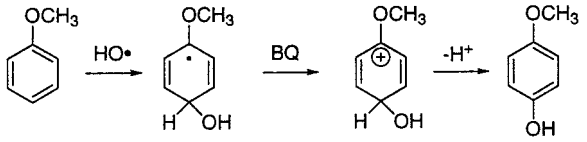

The observed isotopic selectivities of 0.94 and 0.98 for formation of **4** and **5** (entry 6, Table 2) now reflect the expected inverse secondary isotope effect, or at worst, no isotope effect. This result not only makes sense within our own system, but supports the hypothesis of von Sonntag even under his distinctly different conditions.[55] It also gives us a basis for understanding the slightly different selectivities for **4** and **5** under normal photocatalytic conditions, i.e., that the competition between the HOO• elimination and further oxygen trapping is slightly altered by the position of the substituents.

Product Distributions. The predominance of *ortho* and *para* hydroxylation over *meta* is readily understood from the electron donating ability of the methoxy group and the electrophilicity of HO•.[33,34,37] The same predomination of *ortho* and *para* attack should be observed over *ipso*, but phenol is observed in high proportion at low pH. In fact, the overall pH dependence of the product distribution is dramatic. Qualitatively similar pH trends are observed for all three oxidation methods, in that products **2** and **3** predominate at low pH, but hydroxylation products are more important at higher pH.

Scheme 3 shows a plausible explanation for the dramatic change in (**2** + **3**)/(**4** + **5** + **6**) with pH. Acid-promoted dehydration of adducts such as **12** has been proposed in the

Scheme 3

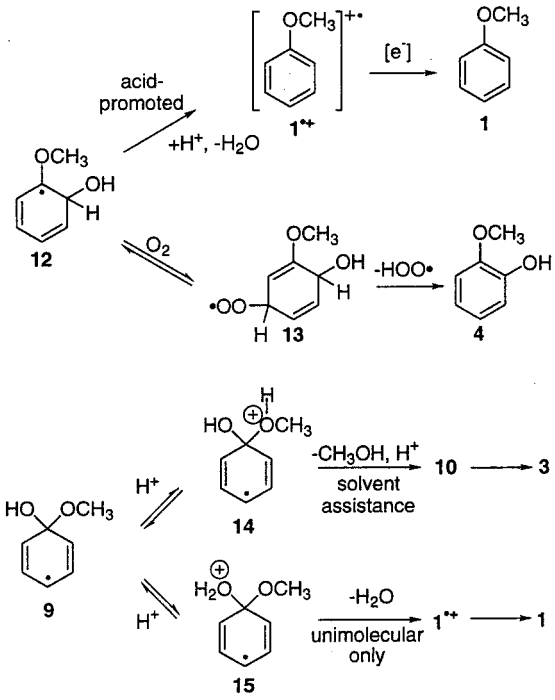

radiolysis literature.[32,35,57,58] Protonation and dehydration of **12** gives the relatively stable radical cation **1**•+, which recovers an electron from other easily oxidizable species. This serves as an inhibition of formation of the hydroxylation products because it competes with the oxygenation route to hydroxylation products. By contrast, acid-promoted decomposition of **9** (the *ipso*-attack precursor to phenol formation) would likely lead mainly to **10** because of the easier decomposition of **14** as compared to **15**. Thus, the ratio of **3**-^{16}**O** to **4** should increase at low pH, as it does. At pH 1 (entry 1, Table 1), the quantity of phenol attributable to *ipso* attack is approximately 10 times greater than the sum of **4** and **5**, compared to a ratio of about 1:4 at pH 7 (entry 4). It seems unreasonable to attribute this to changing selectivity of the initial attack. However, it is also clear that this scheme is a simplification of the entire suite of reactions that occur. The falloff in **4** and **5** does not appear to be linear with $[H^+]$. Indeed, the overall rate of decomposition of **1** slows approximately linearly with pH (not $[H^+]$!). Nonetheless these reactions provide a framework for understanding the observed selectivities and changes thereof.

Conclusions

The gross product distributions in the photocatalytic degradation of anisole follow trends observed in both radiolysis and Fenton conditions. This is taken to show that the major reaction channel for anisole under photocatalytic degradation is hydroxyl-like chemistry rather than electron transfer.

The use of ^{18}O-labeled anisole (**1**-^{18}**O**) has revealed that the TiO_2-mediated conversion of anisole to phenol occurs competitively by two major classes of mechanisms involving *ipso* attack and degradation of the methyl group. This implies that photocatalytic degradation of related aromatic species may result in the release of the alkoxy portion of aryl alkyl ethers before complete degradation of the alkyl group. Similarly, both Fenton and $H_2O_2/h\nu$ show both modes of attack.

(57) O'Neill, P.; Steenken, S.; Schulte-Frohilinde, D. *J. Phys. Chem.* **1975**, *79*, 2773−2779.
(58) Land, E. J.; Ebert, M. *Trans. Faraday Soc.* **1967**, *63*, 1181−1190.

Isotopic selectivities (H vs D) of about 2.7 were obtained for the conversion of anisole to phenyl formate under photocatalytic, Fenton, and oxygenated H_2O_2 photolysis conditions. This was attributed to a primary kinetic isotope effect on the abstraction of a methyl hydrogen. A more complex explanation is required for the selectivities observed for hydroxylation of anisole. Any measurable kinetic isotope effect on addition of hydroxyl to the aromatic ring ought to be less than 1.00; the observation of selectivities of the order of 1.3 can be rationalized if there is a branch point in the mechanism in which the competing pathways have different kinetic isotope effects. The one proposed here, and supported by experiments in which BQ replaces O_2 in photocatalytic degradation, pits an isotope-dependent loss of $HOO^{\bullet}$ against isotope independent trapping of the same intermediate with a second molecule of O_2.

Acknowledgment. The financial support of the NSF in the form of a CAREER grant is gratefully acknowledged.

Supporting Information Available: A table of degradation rates vs pH, a table showing all the concentration ratios used and reaction times for the isotopic selectivities, and an explanation of how the anticipated H/D selectivity of 1.3 in the TiO_2 degradation with BQ is obtained (PDF). This material is available free of charge via the Internet at http://pubs.acs.org.

JA994030H